A Multi-objective Optimization Model for the Quantification of Flexibility in a Large Business Park

Panda, Nanda Kishor; Paterakis, Nikolaos G.

DOI
10.1109/SEST50973.2021.9543270

Publication date
2021

Document Version
Final published version

Published in
2021 International Conference on Smart Energy Systems and Technologies (SEST)

A Multi-objective Optimization Model for the Quantification of Flexibility in a Large Business Park

Nanda Kishor Panda[1], Nikolaos G. Paterakis[2]
Dept. of Electrical Engineering, Eindhoven University of Technology, The Netherlands
Email: [1]nkpanda97@gmail.com, [2]n.paterakis@tue.nl

2021 International Conference on Smart Energy Systems and Technologies (SEST) | 978-1-7281-7660-4/21/$31.00 ©2021 IEEE | DOI: 10.1109/SEST50973.2021.9543270

***Abstract*—Demand-side management (DSM) is an effective way to strengthen the present power system's reliability and security with increasing penetration of renewable energy generations. With the fusion of information technology, present-day loads are getting smarter with their ability to modulate the power and control their switching operations in response to signals. The benefits get multiplied when flexibility is planned for a cluster of consumers having a similar load profile. In this paper, a framework based on mixed-integer linear programming (MILP) is developed to quantify flexibility in a large business park with little historical time series data access. The proposed mathematical model considers smart loads such as heat pumps, electric vehicle (EV) charging stations, a centralized energy storage system and renewable energy sources such as photovoltaic power. The quantification of flexibility is cast as a bi-objective optimization problem, which is solved by approximating the set of Pareto-efficient solutions using the epsilon-constraint method. Based on the developed optimization model, numerical simulations across one year with a time step of one hour are performed. The projected yearly monetary saving ranges from 1.5% to 30.8 %, and maximum peak shavings range from 9.6% to 61.4% for different capacities of centralized energy storage.**

***Index Terms*—Demand-side management, flexibility, multi-objective optimization, smart grid**

I. Introduction

The stress on the current electrical grid is increasing exponentially with the increasing electrification of new sectors. Since 2018, renewable energy sources are the largest contributor to the energy production mix for the European Union [1]. The intermittent nature of renewable energy sources such as solar and wind energy systems make the transition from a conventional power grid to a 100% renewable grid very challenging [2]. Demand-side management (DSM) is a promising solution to renewable integration problems. Using flexibility to shift and modulate load is one of the DSM approach, which can ensure cost-effective and reliable electricity to consumers [3]. As employing collective flexibilities in a community incurs a considerable amount of investment, proper quantification and identification of flexibility is often needed [4]. This process usually requires a significant amount of data and the development of complex mathematical models.

Heating and cooling systems can offer flexibility by varying the set-points of temperature, which is verified in two different residential buildings as test cases [5]. Many authors have developed a mixed-integer linear programming (MILP) based framework for optimizing flexibility specific to the residential sector, which has proved efficient in promoting energy neutrality and peak shaving [6], [7]. Authors in [8] propose a unified and generic framework for modelling flexibility applied to any smart grid setting. Various electrical flexibility categories such as Open, Buffering, Time-window and Storage flexibility have been discussed in [9].

After identifying potential flexibility in a project, it is only logical to look for ways to assess the efficiency and usability of the identified flexibility. A three-tier approach of assessing flexibility serving purposes such as operational planning and stochasticity with varying degrees of complexity to simple visual comparison has been proposed by the International Renewable Energy Agency (IRENA) [10]. Tier 3 analysis is the most detailed and robust assessment approach available, which provides a quantitative result on load, generation and storage needs. For the business park that is used as a case study, in this case, the tier 3 approach is best suited to predict real flexibility potential and savings for various stakeholders. Table I shows two other business parks in the Netherlands, sharing similar energy-neutral goals as the business park under consideration [11]–[14].

II. Research question and Background

The main research question addressed in this paper is "Can electrical flexibility induce considerable savings for various stakeholders of a large commercial space?". The above question is investigated first by identifying suitable sources of flexibility in a large business park such as heat pumps, electric vehicle (EV) charging stations and a centralized battery equipped with a battery management system (BMS) and then present a quantitative model to forecast savings from flexibility considering present and future scenarios.

This paper considers the case of a large business park situated in Eindhoven, the Netherlands, having a considerable amount of photovoltaic (PV) installed, the energy of which is fed back into the utility grid using the SDE+ scheme outlined by the Netherlands Enterprise Agency (RVO) [15]. Currently, solar generation is not used optimally within the buildings, leading to overstretched distribution lines during the collective peak solar energy production.

TABLE I
BUSINESS PARKS WITH SUSTAINABILITY GOALS

Name	Location	Energy sources	Electrical infrastructures	Sustainability goals
A1 Business Park	Deventer	• Wind turbines • Photovoltaics • Biomass boilers	• Own low voltage electrical network	• Reduction in transport tariff • Collective peak reduction
Duiven Business Park	Duiven	• Waste to heat plant with ASES[a] • Photovoltaics • Wind turbines	• District heating network • Distributed generations are directly connected to the utility grid	• Achieve energy neutrality by 2050

[a]Aquifer Seasonal Energy Storage.

Though a large number of works have been done earlier with regards to flexibility quantification in the residential sector and user-specific cases, very little work exists for commercial spaces. Through this paper, the authors aim to bridge the above research gap by presenting a quantitative flexibility model for commercial spaces, which has been validated by data from a large business park.

III. DATA MODELLING

A MILP model is proposed to quantify the flexibility in the business park. To simulate the whole setup, a concrete model approach is chosen, considering multiple sets of the input parameters. The time-series data of all the input parameters are deduced from available yearly data, eliminating the need for a large amount of historical time-series data.

The hourly temperature profile is obtained from the Royal Netherlands Meteorological Institute (KNMI) for the year 2018 from 1st of January till 31st of December [16]. Equation (1) uses the scaling factor (SF) to generate realistic electrical load profiles of the buildings from the Standard Load Profiles (SLP) provided by Open Energy Information (OpenEI) in association with National Renewable Energy Laboratory (NREL).

$$\text{SF} = \frac{\text{Average consumption of building [kWh/day]}}{\text{Average consumption of SLP [kWh/day]}} \tag{1}$$

Due to the huge influence of climate on energy consumption, "Köppen climate classification" is used to first classify the estate as a "cfb" zone, which denotes an oceanic climate [17]. Then different SLPs are used depending upon the size, type and occupancy of the buildings. Thermal load profiles are also modelled similar to electrical load profiles using SLPs from Open Power System Data [18]. Space cooling profiles crucially contribute to each building's energy demand. The major challenge when applying the cooling degree days approach to calculate hourly profile is the lack of cooling demand data [19]. For generating hourly space cooling load profiles, a base case template of cooling load is taken from "CityBes" [20], [21]. All the buildings inside the business parks are equipped with ground source heat pumps, which use groundwater as the source of heat for heating in winter or as a sink to cool the building during summer [22]. As the Coefficient of performance (CoP) varies with outside temperature, the CoP of the heat pumps in heating mode is taken as the historical hourly average CoP for ground source heat pumps with radiator, provided by Open Power System Data [18]. However, during the cooling mode, the CoP is assumed to be constant.

$$\text{CF} = \frac{\text{Total yearly generation [kWh]}}{\text{Theoretical max power * 365*24 [kWh]}} \tag{2}$$

PV generation profile is calculated for each hour of the year 2018 using "PVWatts", which is an interactive open-source solar modelling software provided by NREL [23]. The system losses are assumed to be capped at 12.3%. The Capacity Factor (CF) for the calculation is found to be 10.4% from historical data using (2).

IV. FORMULATION OF THE MILP MODEL

A. Objective functions

The symbols used in the MILP model are defined in Table II. Equations (3) and (4) define the objective functions, which are minimized over the whole year (8760-time steps). The first objective function assumes that only the electricity imported from the utility grid is of monetary value and minimizes all electrical load's operating costs by optimizing the heat pump's power output. The second cost function accounts for self-sufficiency, which limits dependency on the utility grid and supports peak shaving.

$$CF_1 = \text{minimize}\left[\sum_t \left(W_t^{grid} \cdot \lambda_t\right)\right] \tag{3}$$

$$CF_2 = \text{minimize}\left[\underset{t\in T}{max}\ |W_t^{grid}|\right] \tag{4}$$

B. Constraints

The first set of constraints defined by (6) and (7) reflect the heat balance inside the buildings. The temperature inside the building is calculated assuming that the instantaneous heat content inside a building filled by homogeneous air depends on the heat supplied by the heat pump(Q_t^{hp}), internal heat gain (Q_t^{int}) due to solar insolation, occupancy, lighting, etc. and heat losses (Q_t^{ext}) by ventilation and inherent thermal property of the building as given in (5) [24], [25]. C is the heat capacity of air given by $C_p \rho_{air} V_{building}$ in [kW/°C]. The minimum and maximum allowed temperature inside the buildings during maximum occupancy is decided according to the recommended temperature limits given by Dutch heat pump installation companies as given in (7) [26]. To make the optimum use of heat pumps, temperature settings also depends

TABLE II
NOMENCLATURES

Indices and Sets	
t(**T**)	Set of all time slices with each time step equals to 1 hour; $t \in \mathbf{Z}^+ : 1 \leq t \leq 8760$.
i(**I**)	Set of all buildings; $i \in \mathbf{Z}^+ : 1 \leq i \leq 23$.
s(**S**)	Set of all electric vehicles(EVs); $s \in \mathbf{Z}^+ : 1 \leq s \leq 100$.
Input Parameters	
A_i^x	Surface area of i^{th} building ($x = \{\text{glass, roof, facade}\}$) $[m^2]$.
U_i^x	Thermal transmittance of i^{th} building ($x = \{\text{glass, roof, facade}\}$) $[\frac{W}{m^2 \circ C}]$.
V_i	Volume of i^{th}building $[m^3]$.
$P_i^{hp,max}$	Rated power input of the heat pump installed in i^{th} building $[kW]$.
$OL_{t,i}$	Non-flexible electrical demand of i^{th} building at t hour $[kW]$.
$O_{t,i}$	Occupancy level inside i^{th} building at t hour.
γ_t	CoP of all heat pumps at hour t.
SG_t	Collective solar generation of all buildings at hour t $[kW]$.
T_t^{out}	Outside temperature at hour t $[^\circ C]$.
λ_t	Day-ahead price of electricity at hour t $[€/kWh]$.
$P^{Bat,max}$	Maximum charging/discharging power of the centralized battery $[kW]$.
$\chi^{Bat,x}$	Max, min or initial SoE of centralized battery respectively ($x = \{max, min, ini\}$) $[kWh]$.
$P_s^{EV,max}$	Maximum charging/discharging power of the s^{th} EV $[kW]$.
$\chi^{EV,x}$	Max, min and initial SoE of s^{th} EV respectively ($x = \{max, min, ini\}$) $[kWh]$.
w_t	Binary parameter for separating weekday ($w_t = 1$) and weekend ($w_t = 0$).
τ_t	Time stamp for the hour of a day in 24 hour format.
Variables	
$W_t^{grid,x}$	Positive, negative and net grid import respectively at hour ($x = \{' ', pos, neg\}$) t $[kW]$.
$P_{t,i}^{hp,x}$	Power input to the heat pumps at hour t in the i^{th} building for heating or cooling respectively ($x = \{heat, cool\}$). $[kW]$.
$P_t^{Bat,x}$	Charging or discharging power of the centralized battery at hour t respectively ($x = \{ch, dis\}$) $[kW]$.
$P_{t,s}^{EVt,x}$	Charging or discharging power of s^{th} EV at hour t respectively ($x = \{ch, dis\}$) $[kW]$.
χ_t^{Bat}	SoE of the centralized battery at hour t. $[kWh]$.
$\chi_{t,s}^{EV}$	SoE of s^{th} EV at hour t $[kWh]$.
u_t^{Bat}	Binary variable indicating whether the centralized battery is charging(=1) or discharging(=0) at hour t .
$u_{t,i}^{hp}$	Binary variable indicating whether heat pump in i^{th} building is heating(=1) or cooling (=0) at hour t.
$u_{t,s}^{EV}$	Binary variable indicating whether s^{th} EV is charging (=1) or discharging (=0) at hour t.
$T_{t,i}^{in}$	Temperature inside i^{th} building at hour t $[^\circ C]$.
Ω	Auxiliary variable used to linearize CF_2 $[kW]$.
f^1, f^2	Auxiliary variable equal to value of CF_1 and CF_2 respectively $[€, kW]$.
ϵ, ξ	Auxiliary variables used to implement augmented epsilon constraint.
Physical Constants	
Δt	Duration of time-step taken as 1[hr].
ρ_{air}	Density of air taken as 1.007 $\left[\frac{kg}{m^3}\right]$.
S_{air}	Specific heat of air at constant pressure taken as 1.19 $\left[\frac{kJ}{\circ Ckg}\right]$.
f	Factor accounting for internal and solar heat gains taken as $f = 0.003 \quad \forall\, T_t^{out} > 22^\circ C$ or $f = 0.075 \quad \forall\, T_t^{out} \leq 22^\circ C$.

on the occupancy level($O_{t,i}$) of each building, which varies from 8 to 100%.

$$C\frac{dT_t^{in}}{dt} = Q_t^{ext} + \underbrace{f * Q_t^{thermal}}_{Q_t^{int}} \pm Q_t^{hp} \tag{5}$$

For simplicity, heat gain/loss by ventilation is neglected in the simulation study. Furthermore, the internal heat generation can be equated to a factor of the thermal heat generated [27].

$$T_{t,i}^{in} = \begin{cases} T_0^{in} + \alpha_i \left[(1 + f\beta_i)(T_t^{out} - T_0^{in})\right] \\ \qquad\qquad \forall t \in \mathbf{T} = 0, i \in \mathbf{I} \\ T_{t-1,i}^{in} + \alpha_i[(1 + f\beta_i)(T_{t-1}^{out} - T_{t-1,i}^{in}) + \\ \qquad \Gamma_{t-1} P_{t-1,i}^{hp,heat} - 11 * P_{t-1,i}^{hp,cool}] \\ \qquad\qquad \forall t \in \mathbf{T} > 0, i \in \mathbf{I} \end{cases} \tag{6}$$

$$T_{t,i}^{in} \in \begin{cases} Skip & \forall\, t \in \mathbf{T} = 1, i \in \mathbf{I} \\ [20, 24] & \forall\, O_{t,i} = 1.00, t \in \mathbf{T} > 1, i \in \mathbf{I} \\ [19, 25] & \forall\, O_{t,i} = 0.80, t \in \mathbf{T} > 1, i \in \mathbf{I} \\ [18, 26] & \forall\, O_{t,i} = 0.20, t \in \mathbf{T} > 1, i \in \mathbf{I} \\ [17, 27] & \forall\, O_{t,i} = 0.10, t \in \mathbf{T} > 1, i \in \mathbf{I} \\ [16, 28] & \forall\, O_{t,i} = 0.08, t \in \mathbf{T} > 1, i \in \mathbf{I} \end{cases} \tag{7}$$

The constants β_i and α_i depend on the A_i^x and U_i^x of each building as given in (8) and (9). The values of $U_i^{x=facade,roof,glass}$ are assumed to be identical for all buildings and take the values as 0.35, 0.30 and 0.30, respectively.

$$\beta_i = U_i^{glass} A_i^{glass} + U_i^{roof} A_i^{roof} U_i^{facade} A_i^{facade} \tag{8}$$

$$\alpha_i = \frac{\Delta t}{\rho_{air} V_i S_{air}} \tag{9}$$

Constraint (10) balances the energy flow in and out of the whole property at each time step.

$$W_t^{grid} + SG_t + P_t^{Bat,dis} - P_t^{Bat,ch} + \sum_s \left(P_{t,s}^{EV,dis} - P_{t,s}^{EV,ch}\right) = \sum_i \left(P_{t,i}^{hp,heat} + P_{t,i}^{hp,cool} + OL_{t,i}\right) \;\forall\, t \in \mathbf{T}, i \in \mathbf{I} \tag{10}$$

Conventional heat pumps can only turn on and operate at their constant nominal power, leading to frequent switching when using them to enrich flexibility. The heat pump's input power is modelled as a continuous variable using constraints (11) and (12), which can be achieved by using variable frequency drives that are getting popular in practice [28]. Along with adequate control of the heat pump output, these type of heat pumps can reduce a very high starting current and increase efficiency [29].

$$0 \leq P_{t,i}^{hp,heat} \leq P_i^{hp,max} u_{t,i}^{hp} \qquad \forall\, t \in \mathbf{T}, i \in \mathbf{I} \tag{11}$$

$$0 \leq P_{t,i}^{hp,cool} \leq P_i^{hp,max}(1 - u_{t,i}^{hp}) \quad \forall\, t \in \mathbf{T}, i \in \mathbf{I} \tag{12}$$

Constraints (13)-(16) model the centralized battery as if it is connected centrally with all the buildings. It is assumed to

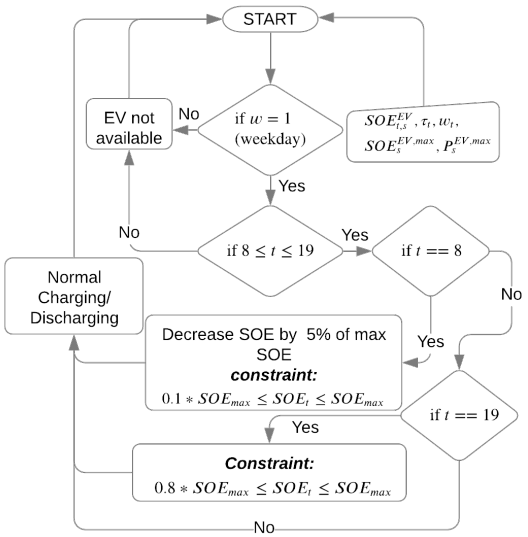

Fig. 1. Charging and discharging process for the electric vehicles connected to charging stations inside the business park.

have the required capacity to supply peak power for six hours while discharging continuously.

$$\chi_t^{Bat} = \begin{cases} \chi^{Bat,ini} + \eta^{Bat} P_t^{Bat,ch} - \dfrac{P_t^{Bat,dis}}{\eta^{Bat}} & t = 1 \\ \chi_{t-1}^{Bat} + \eta^{Bat} P_t^{Bat,ch} - \dfrac{P_t^{Bat,dis}}{\eta^{Bat}} & \forall t \geq 1 \end{cases} \tag{13}$$

$$\chi^{Bat,min} \leq \chi_t^{Bat} \leq \chi^{Bat,max} \qquad \forall\, t \in \mathbf{T} \tag{14}$$

$$P_t^{Bat,ch} \leq P^{Bat,max}(u_t^{Bat}) \qquad \forall\, t \in \mathbf{T} \tag{15}$$

$$P_t^{Bat,dis} \leq P^{Bat,max}(1 - u_t^{Bat}) \qquad \forall\, t \in \mathbf{T} \tag{16}$$

It is assumed that there is a fleet of one hundred plug-in EV charging outlets, each having the capacity of a maximum of 11 kW output (3 phase, 16 A) [30]. To model the EV charging station, one hundred EVs with different battery capacity are considered. The mix of a hundred four-Wheeler is chosen by comparing the most popular cars in the Netherlands. The charging and discharging process for a single day for each EV is modelled using constraints (17)-(21), which follow the process shown in Fig. 1. For realistic simulation, each EV is assumed to be available in the premises of the business park only during 8:00 am to 7:00 pm during weekdays. Besides, the initial state of energy ($S_s^{EV,ini}$) for each EV is randomly initialized.

$$\chi_{t,s}^{EV} = \begin{cases} \chi_{t-1,s}^{EV} - \delta_t^{EV} \chi_s^{EV,max} + \eta^{EV} P_{t,s}^{Bat,ch} - \dfrac{P_{t,s}^{EV,dis}}{\eta^{EV}} & \forall\, t \in \mathbf{T} > 8 \\ \chi_s^{EV,ini} & \forall\, t \in \mathbf{T} \leq 8 \end{cases} \tag{17}$$

$$P_{t,s}^{EV,ch} \begin{cases} \leq u_{t,s}^{EV} P_s^{EV,max} & \forall\, 8 \leq \tau_t \leq 19 \wedge w_t = 1 \\ = 0 & \forall\, (\tau_t \leq 8 \wedge \tau_t \geq 19) \wedge w_t = 0 \end{cases} \tag{18}$$

$$P_{t,s}^{EV,dis} \begin{cases} \leq (1 - u_{t,s}^{EV}) P_s^{EV,max} & \forall\, 8 \leq \tau_t \leq 19 \vee w_t = 1 \\ = 0 & \forall\, (\tau_t \leq 8 \wedge \tau_t \geq 19) \wedge w_t = 0 \end{cases} \tag{19}$$

The car usage beyond the premises of the business park is incorporated in the model by introducing a time-dependent variable (δ_t^{EV}) which reduces the SOE of each vehicle by 5% of their maximum state of energy every day at 8:00 hours as given by (20)-(22).

$$\delta_t^{EV} = \begin{cases} 0.05 & \forall \quad \tau_t = 8 \\ 0.05 & \forall \quad \tau_t \in [1, 24] - \{8\} \end{cases} \tag{20}$$

$$0.1 S_{t,s}^{EV} \leq \chi_s^{EV,max} \quad \forall\, t > 8 \wedge (\tau_t \in [1, 24] - \{19\}) \tag{21}$$

$$0.8 S_{t,s}^{EV} \leq \chi_s^{EV,max} \quad \forall\, t > 8 \wedge (\tau_t = \{19\}) \tag{22}$$

The objective function (4) related to self-sufficiency is trivially linearized by introducing an additional variable (Ω_t) and adding extra constraints given in (23)-(26) [31].

$$\text{minimize} \quad \boldsymbol{\Omega} \tag{23}$$

$$\text{s.t.:} \quad W_t^{grid} = W_t^{grid,pos} - W_t^{grid,neg} \tag{24}$$

$$W_t^{grid,pos}, W_t^{grid,neg} \geq 0 \tag{25}$$

$$\Omega \geq W_t^{grid,pos} \text{ and } \Omega \geq -W_t^{grid,neg} \tag{26}$$

C. Solving of the multi-objective optimization

The augmented ϵ-constraint (AUGMECON) is used to solve the formulated multi-objective optimization [32]. Equations (27)-(30) help to implement the AUGMECON method efficiently.

$$\text{minimize} \ \left[f^1 - \Delta * \xi\right] \tag{27}$$

$$\text{s.t.:} \quad f^2 + \xi = \epsilon \tag{28}$$

$$f^1 = \left[\sum_t \left(W_t^{grid} \cdot \lambda_t\right)\right] \quad \forall\, i \in \mathbf{I}, t \in \mathbf{T} \tag{29}$$

$$f^2 = \Omega \tag{30}$$

The value of Δ is chosen as 10^{-5}, and the values of ϵ are iterated through the grid points whose lower and upper range are derived from the lexicographic optimization payoff table [32]. The process of obtaining the payoff table and the flowchart for applying AUGMECON is shown in Fig. 2. From the generated Pareto-front shown in Fig. 3, the best-case scenario is chosen to calculate the maximum savings in total system cost (TSC) and total grid import.

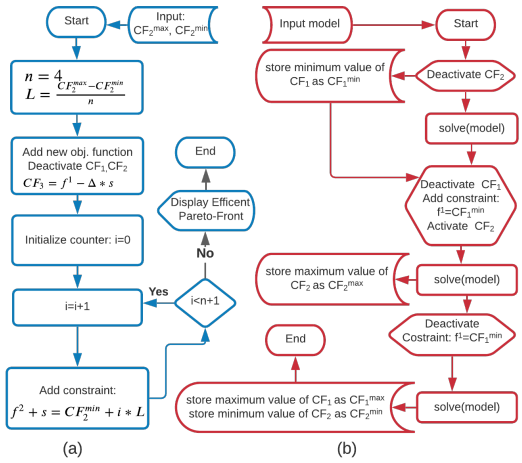

Fig. 2. (a) Flowchart for the implementation of AUGMECON, (b)Flowchart for the lexicographic optimization to obtain desired payoff table.

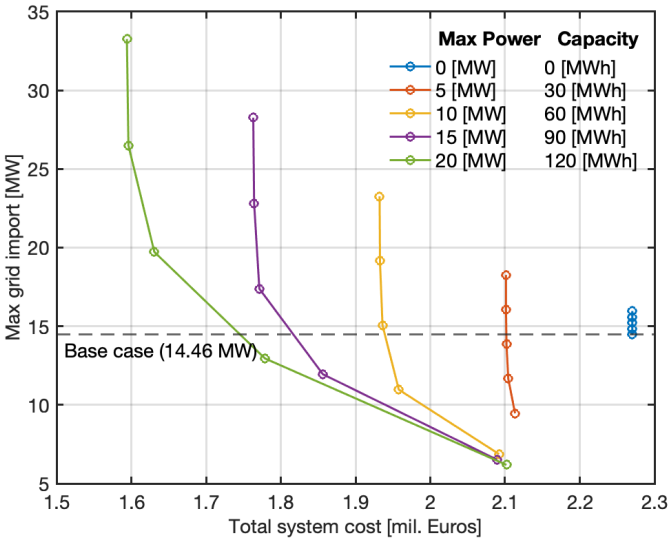

Fig. 3. Pareto front for different battery sizes.

V. Results and Analysis

The proposed MILP model is implemented in Python using the Pyomo package and then solved using the "Gurobi" solver on a 2.6 GHz 6-Core Intel i7 Macintosh system with a relative "MI Gap" of 0.5 %. Hourly samples for the year 2018 are used as input parameters. The original load profile derived from the annual electrical consumption data is taken as the base case. According to the base case, the TSC amounts to €2.3045 million, and the maximum grid import stands at 16.01 MW.

The total yearly consumption of the heat pumps for heating and cooling without flexibility (base case) amounted to 1747.7692 MWh. By leveraging user comfort by expanding the temperature margin, the yearly consumption reduced to 1021.8993 MWh. This shows a saving of 725.8699 MWh annually. The variation of the electrical power output of the heat pumps for both the cases is plotted in Fig. 4 along with the outside temperature. By assuming a yearly average price of 0.052 €/kWh, approximately €37745 can be saved annually.

TABLE III
Relative Savings for Various Battery Capacities

Battery Power [MW]	Battery Capacity [MWh]	TSC [mil. €]	TSC Relative [%]	Max Grid Import [MW]	Max Grid Import Relative [%]
0	0	0.0343	1.5	1.546	9.6
1	6	0.0685	3.0	2.55	15.9
5	30	0.2033	8.8	6.546	40.9
10	60	0.3722	16.2	9.141	57.1
15	90	0.5414	23.5	9.499	69.3
20	120	0.7103	30.8	9.825	61.4

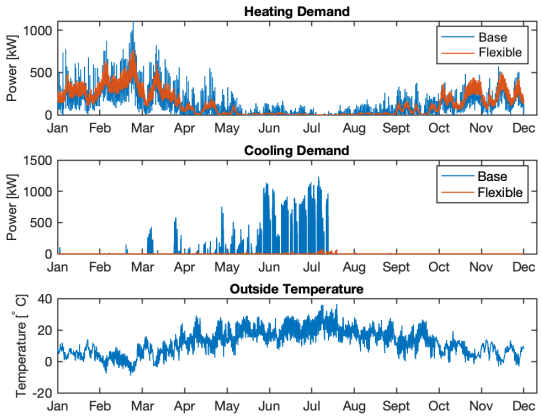

Fig. 4. Variation of power usage of heat pumps with and without flexibility.

The MILP model is simulated for battery capacities in the range of 0-120 MWh to optimize the centralized storage size. The TSC in euros is then compared with the base scenario, as given in Table III. Only with flexibility and optimization, the TSC is reduced by €40000. By increasing the battery capacity, the yearly TSC decreases. However, to decide the optimal battery capacity, maximum grid import and export need to be validated as they are one of the factors affecting the bottleneck at the local substation. Hence by trading off between the TSC and maximum grid import, a battery with a capacity of 6 MWh is ideal for the current situation.

For the entire year, 44.8 MWh of electrical energy is used to charge the entire fleet of a hundred EVs. Assuming an average of 0.191 kWh/km, a total of 2,34,554.97 km can be covered by all the cars in total. Compared to the CO_2 emissions by petrol engines, this has an indirect CO_2 reduction of 51.60 tons/year [33], [34].

VI. Conclusion

The primary findings of this study are as follows:

- The initial assessment indicates the potential for significant monetary savings for the various stakeholders.
- Savings increases when flexibility among clusters of smart loads is considered instead of isolated loads.
- A trade-off between operating cost and maximum grid import has to be identified in order to decide the optimal capacity of centralized storage.

Apart from monetary savings, the following business cases may be of interest to the various stakeholders of the property:

- The *business park property owner* can act as an aggregator to facilitate flexibility within the companies. Other

business models which can be applied include energy as service and pay-as-you-go models.

- The direct benefits to the *Distribution System Operators (DSOs)* include peak shaving and better congestion management during peak hours. It also opens the possibility of explicit flexibility for its consumers in the future.
- The *local government* has the advantage of the solid implementation of the climate agreement through this project utilizing cutting back natural gas and CO_2 usage along with promoting renewable energy. The business park can be taken up as an example model for other business parks.
- *Companies inside the business park* receive the most direct benefit. Efficient energy management translates into yearly cost savings. The companies can use low investment flexible loads such as EV charging to offer their employers incentives and promote EVs. This indirectly helps the company be energy neutral and promote its corporate social responsibility activities.

REFERENCES

[1] "Statistics Explained and Data", "Electricity and heat statistics," p. 13, 2020. [Online]. Available: https://ec.europa.eu/eurostat/statisticsexplained/

[2] C. F. Heuberger and N. Mac Dowell, "Real-World Challenges with a Rapid Transition to 100% Renewable Power Systems," pp. 367–370, 3 2018.

[3] IRENA(2019), "Demand-side flexibility for power sector transformation," International Renewable Energy Agency, Abu Dhabi, Tech. Rep., 2019.

[4] E. M. Ländner, A. Märtz, M. Schöpf, and M. Weibelzahl, "From energy legislation to investment determination: Shaping future electricity markets with different flexibility options," *Energy Policy*, vol. 129, no. March, pp. 1100–1110, 2019. [Online]. Available: https://doi.org/10.1016/j.enpol.2019.02.012

[5] J. Le Dréau and P. Heiselberg, "Energy flexibility of residential buildings using short term heat storage in the thermal mass," *Energy*, vol. 111, pp. 991–1002, 9 2016.

[6] B. Mattlet and J.-C. Maun, "Assessing the benefits for the distribution system of a scheduling of flexible residential loads," in *2016 IEEE International Energy Conference (ENERGYCON)*. Leuven, Belgium: IEEE, 2016, pp. 1–6.

[7] J. Kiljander, D. Gabrijelčič, O. Werner-Kytölä, A. Krpič, A. Savanović, . Stepančič, V. Palacka, J. Takalo-Mattila, and M. Taumberger, "Residential Flexibility Management: A Case Study in Distribution Networks," *IEEE Access*, vol. 7, pp. 80 902–80 915, 2019.

[8] L. Barth, N. Ludwig, E. Mengelkamp, and P. Staudt, "A comprehensive modelling framework for demand side flexibility in smart grids," *Computer Science - Research and Development*, vol. 33, no. 1-2, pp. 13–23, 2018.

[9] B. Roossien, "Mathematical quantification of near real-time flexibility for Smart Grids," Energy research Centre of the Netherlands (ECN) 1, Tech. Rep., 2020. [Online]. Available: http://www.flexines.org/publicaties/eindrapport/BIJLAGE14a.pdf

[10] IRENA, "Power system flexibility for the energy transition. Part II: IRENA Flextool methodology," International Renewable Energy Agency, Tech. Rep. December, 2018. [Online]. Available: https://www.irena.org/publications/2018/Nov/Power-system-flexibility-for-the-energy-transition

[11] "Cleantech Region - Climate-KIC." [Online]. Available: https://www.climate-kic.org/partners/cleantech-region/

[13] D. Ronde, "Two sides of the smart grid coin a holistic performance review of smart microgrid project A1 Deventer," Eindhoven University of Technology, Tech. Rep., 2016.

[12] Netherlands Enterprise Agency, "Modular smart grid for business parks Innovation programme commissioned by the ministry of Economic Affairs," Innovation programme commissioned by the ministry of Economic Affairs , Tech. Rep., 2015. [Online]. Available: www.rvo.nl/intelligentenetten

[Online]. Available: https://research.tue.nl/en/studentthesis/two-sides-of-the-smart-grid-coin(9e474f1d-1d27-43a9-b40c-9cebb36dc643).html

[14] J. Boon, "Designing a sustainable and energy-neutral business park," University of Twente, Tech. Rep., 2016. [Online]. Available: https://essay.utwente.nl/71920/

[15] "Dutch Renewable Energy Support Scheme (SDE+)," The Netherlands Enterprise Agency, Tech. Rep. [Online]. Available: https://www.ecn.nl/collaboration/sde/index.html

[16] "KNMI - Hourly weather data for the Netherlands - Download." [Online]. Available: http://projects.knmi.nl/klimatologie/uurgegevens/selectie.cgi

[17] J. Ascencio-Vásquez, K. Brecl, and M. Topič, "Methodology of Köppen-Geiger-Photovoltaic climate classification and implications to worldwide mapping of PV system performance," *Solar Energy*, vol. 191, pp. 672–685, 10 2019.

[18] "Open Power System Data A platform for open data of the European power system." [Online]. Available: https://open-power-system-data.org/

[19] D. Conolly, D. Drysdale, K. Hansen, and T. Novosel, "Creating Hourly Profiles to Model both Demand and Supply," Intelligent Energy Europe Programme of the European Union, Tech. Rep., 2015. [Online]. Available: https://stratego-project.eu

[20] "CityBES." [Online]. Available: https://citybes.lbl.gov/

[21] Y. Chen, T. Hong, X. Luo, and B. Hooper, "Development of city buildings dataset for urban building energy modeling," *Energy and Buildings*, vol. 183, pp. 252–265, 1 2019.

[22] Natural Resource Canada's Office of Energy Efficiency, *Heating and cooling with a heat pump*. Natural Resources Canada, 2004.

[23] National Renewable Energy Laboratory (NREL), "PVWatts Calculator." [Online]. Available: https://pvwatts.nrel.gov/

[24] A. Soares, . Gomes, and C. H. Antunes, "A Discussion of Mixed Integer Linear Programming Models of Thermostatic Loads in Demand Response," in *Advances in Energy System Optimization-Proceedings of the First International Symposium on Energy System Optimization*, ser. Trends in Mathematics, V. Bertsch, A. Ardone, M. Suriyah, W. Fichtner, T. Leibfried, and V. Heuveline, Eds. Springer International Publishing, 2020, ch. 3, pp. 105–122. [Online]. Available: http://link.springer.com/10.1007/978-3-319-51795-7 http://link.springer.com/10.1007/978-3-030-32157-4

[25] V. Ruana, "Fundamentals of Heat and Mass Transfer 7th Edition - Bergman, Lavine, Incropera, DeWitt."

[26] "Gebruikerstips Engeltherm Airconditioning & Warmtepompen." [Online]. Available: https://www.engeltherm.nl/beheer/gebruikerstips/

[27] P. Lubina and M. B. Nantka, "SOURCES OF INTERNAL HEAT GAINS IN BUILDINGS," *Architecture civil engineering environment*, vol. 2, no. 1, pp. 137–142, 2009.

[28] A. Gomes, C. H. Antunes, and J. Martinho, "A physically-based model for simulating inverter type air conditioners/heat pumps," *Energy*, vol. 50, no. 1, pp. 110–119, 2013. [Online]. Available: http://dx.doi.org/10.1016/j.energy.2012.11.047

[29] Y. J. Kim, J. L. Kirtley, Y.-J. Kim, S. Member, L. K. Norford, and J. L. Kirtley, "Modeling and Analysis of a Variable Speed Heat Pump for Frequency Regulation Through Direct Load Control," *IEEE Transactions on Power Systems*, vol. 30, no. 1, pp. 397–408, 2015.

[30] "Understanding Electric Car Charging - Spirit Energy." [Online]. Available: https://www.spiritenergy.co.uk/kb-ev-understanding-electric-car-charging

[31] W. E. Hart, C. Laird, J.-P. Watson, and D. L. Woodruff, *Pyomo Optimization Modeling in Python*, ser. Springer Optimization and Its Applications, P. M. Pardalos and D.-Z. Du, Eds. Boston, MA: Springer US, 2012, vol. 67. [Online]. Available: http://www.springer.com/series/7393 http://link.springer.com/10.1007/978-1-4614-3226-5

[32] G. Mavrotas, "Effective implementation of the ϵ-constraint method in Multi-Objective Mathematical Programming problems," *Applied Mathematics and Computation*, vol. 213, no. 2, pp. 455–465, 2009. [Online]. Available: http://dx.doi.org/10.1016/j.amc.2009.03.037

[33] "Energy consumption of full electric vehicles cheat-sheet - EV Database." [Online]. Available: https://ev-database.org/cheatsheet/energy-consumption-electric-car

[34] "Carbon Footprint & EV Calculator — Ecotricity NZ." [Online]. Available: https://ecotricity.co.nz/electricvehicles/calculator/